Proceedings World Geothermal Congress 2005
Antalya, Turkey, 24-29 April 2005

New Magnetotelluric Response Functions for Geothermal Applications

José M. Romo, Enrique Gómez-Treviño and Ricardo G. Antonio-Carpio

CICESE, División de Ciencias de la Tierra, Ensenada B.C., México

jromo@cicese.mx, egomez@cicese.mx, rantonio@cicese.mx

Keywords: geophysics, magnetotellurics, electromagnetic methods, geothermal exploration, Las Tres Vírgenes, México

ABSTRACT

As geothermal reservoirs usually occur in geologically complex zones, where the physical properties of the rocks have complicated geometrical distributions, the traditional 2-D TE-TM approach for magnetotelluric interpretation severely limits the use of the available information. 3-D inversion using the full tensor information is so far too expensive for standard use, mainly because both the number of model parameters and the number of response functions are too large. In this work we use a new approach, the series and parallel transformation, which transforms the tensor into two complementary impedances and two angular response functions. This new representation of MT responses is valid regardless of dimensionality and, unlike the tensor elements do not depend on rotations of the measuring reference system. The series and parallel impedances play the roll of the TE and TM modes in 2-D situations. In addition, our approach could be an alternative to reduce the number of response functions used in 3-D interpretation. We present applications to field data from Las Tres Vírgenes geothermal field in Mexico.

1. INTRODUCTION

Magnetotelluric method (MT) is based on the fact that the natural time-varying electromagnetic field at the surface of the earth is sensitive to the conductivity distribution at depth. The ability of MT to detect electrical conductivity anomalies in the subsurface, along with its considerable exploration depth, are very useful skills in geothermal exploration, as high-conductivity anomalies are usually associated to high temperatures, saline fluids and hydrothermal alteration caps at the top of many geothermal reservoirs.

The magnetotelluric response function, which connects subsurface electrical conductivity with the electromagnetic fields measured at the surface, is commonly represented by an impedance tensor. This mathematical form summarizes the effect of any system of electric currents flowing in the media. On the other hand, current interpretation tools necessarily rely on simplified models of the earth, which in some way are over constrained by the information provided by the tensor.

A frequently used model assumes the subsurface resistivity as a function of only two dimensions (one horizontal distance and depth). In this 2-D case any system of currents can be decoupled in two perpendicular modes: one of them related with electrical currents flowing along the structure interfaces: TE polarization mode; the other one is associated with current flowing across the structure interfaces: TM polarization mode. Interpretation of MT data in terms of 2D models is naturally based on these TE and TM polarization modes. Standard interpretation algorithms use optimization techniques search for 2-D models able to reproduce the observed MT response (e.g. deGroot-Hedlin and Constable, 1990, 2004; Smith and Booker, 1991; Uchida, 1993; Ogawa and Uchida, 1996; Siripunvaraporn and Egbert, 2000; Rodi and Mackie, 2001).

Because field data inevitably contain 3-D information, a long-standing problem has been the conciliation of entirely general data with over-simplified earth models. Several approaches have been proposed to reduce the four elements of the impedance tensor to a couple of impedances comparable with the TE and TM polarization modes of 2-D models. As geothermal reservoirs usually occur in geologically complex zones, where the physical properties of the rocks have complicated geometrical distributions, a very judicious use of tensor-reduction techniques is necessary. It is common that interpretation is limited to the TM mode, as 2-D modeling easily reproduces it. In contrast, the TE mode of a 2-D model, caused exclusively by inductive effects, is difficult to fit because it is not comparable with the measured impedance along strike, which is certainly affected by galvanic (3-D) effects.

Alternatively, 3-D inversion using the full tensor is so far too expensive for standard use, mainly because both, the number of model parameters and the number of response functions are too large. Functional codes are by Sasaki (1999; 2001), Newman and Alumbaugh (2000), Zhdanov et al. 2000; Uchida and Sasaki (2003).

The approach proposed by Romo et al. (2004), the series and parallel (S-P) transformation, transforms the tensor into two complementary impedances and two angular response functions. This new representation contains information of the whole current system in a general 3-D media, as the full tensor does, but it involves only two impedance functions, series and parallel, which are directly comparable with the TM-TE modes of 2-D models. Moreover, it is also usable in 3-D modeling, along with the angular functions that complete the full representation.

Unlike the tensor elements, S-P impedances do not depend on rotations of the measuring reference system, setting aside the delicate task of pre-selecting structural azimuths. In addition, the S-P impedances are more robust than the original tensor elements, as they are some kind of average of them. Moreover, this averaging naturally reduces any static-shift distortion present in the tensor elements.

In this work we describe the basics of the S-P transformation and apply it to the 2-D inversion of two magnetotelluric profiles in Las Tres Vírgenes geothermal field, in Mexico. The resulting resistivity cross-sections are compared with subsurface geology information provided by several drill-holes in the area.

2. THE IMPEDANCE TENSOR

The magnetotelluric (MT) response function connecting subsurface electrical conductivity with measured electro-

magnetic fields is commonly represented by an impedance tensor

$$\begin{pmatrix} E_x \\ E_y \end{pmatrix} = \begin{pmatrix} Z_{xx} & Z_{xy} \\ Z_{yx} & Z_{yy} \end{pmatrix} \begin{pmatrix} H_x \\ H_y \end{pmatrix} \qquad (1)$$

This mathematical form summarizes the effect of any system of electrical current flowing in the media. In vector notation equation (1) is $\mathbf{E} = \mathbf{Z}\,\mathbf{H}$, where $\mathbf{E}$ and $\mathbf{H}$ are the electric and magnetic fields, and $\mathbf{Z}$ is the impedance tensor.

For ideal 1-D or 2-D media, the full tensor reduces to an off-diagonal form. In the first case, the two resulting elements lead to the same apparent resistivity; and in the second case they lead to two distinctive apparent resistivity functions. One of them is related with electrical current along the structure interfaces: TE polarization mode; the other one associated with current flowing across the structure interfaces: TM polarization mode.

For general 3-D cases, TE and TM polarization modes cannot completely describe the current systems. Thus the response of the subsurface resistivity is spread out in four tensor elements. This fact creates a dilemma: to use the full tensor for 3-D modeling, or to do 2-D modeling providing alternative responses able to describe the 3-D earth in a similar way as TE and TM impedances do for a 2-D earth.

3. S-P TRANSFORMATION

Romo et al. (2004) transform the impedance tensor into four new response functions: two of them are impedances and other two are angular functions. This new set has some interesting properties that overcome some of the limitations the conventional analyses.

Series and parallel transformation of Romo et al. (2004) is based on two basic ideas. The first one consists on formulating a complex transformation able to reduce the 3-D tensor to an off-diagonal form. The second idea consists on combining the reduced impedances in a similar way as the series and parallel equivalents of circuit theory.

Reduction of a general 3-D tensor to a off-diagonal form is achieved by a complex transformation that introduces rotations as well as phase shifts to the electromagnetic fields

$$\mathbf{R}_e\,\mathbf{E} = \mathbf{R}_e\,\mathbf{Z}\;\mathbf{R}_h^{\mathrm{T}}\,\mathbf{R}_h\,\mathbf{H}\;, \qquad (2)$$

where

$$\mathbf{R}_e = \begin{pmatrix} \cos\theta_e & \sin\theta_e \\ -\sin\theta_e & \cos\theta_e \end{pmatrix}\;, \qquad (3)$$

is a unitary matrix with elements given by circular functions of the complex variable $\theta_e = \alpha + i\beta$. $\mathbf{R}_h$ is a similar transformation applied to the magnetic field. The complex argument allows phase shifts in the electromagnetic fields. The transformed impedance reduces to

$$\mathbf{Z}' = \mathbf{R}_e\,\mathbf{Z}\,\mathbf{R}_h^{\mathrm{T}} = \begin{pmatrix} 0 & Z_1 \\ Z_2 & 0 \end{pmatrix}\;, \qquad (4)$$

so that equation (2) transforms to $\mathbf{E}' = \mathbf{Z}'\,\mathbf{H}'$ with $\mathbf{E}' = \mathbf{R}_e\,\mathbf{E}$ and $\mathbf{H}' = \mathbf{R}_h\,\mathbf{H}$.

Solution of equation (4) in terms of θ_e , θ_h, Z_1 and Z_2, transforms the four elements of the original tensor in four new complex parameters: two impedances and two angles

$$\{Z_{xx},\;\; Z_{xy},\;\; Z_{yx},\;\; Z_{yy}\} \Leftrightarrow \{Z_1,\;\; Z_2,\;\; \theta_e,\;\; \theta_h\} \qquad (5)$$

Principal impedances Z_1 and Z_2 are then combined following the series and parallel analogy of circuit theory. In a circuit with resistors in a series array, voltages are added and the result divided by the common current to obtain an equivalent resistance. The transformed electric filed components are added and divided by an appropriate magnetic field to obtain the equivalent series impedance. This is formulated as

$$E_S = \begin{pmatrix} Z_2 & Z_1 \end{pmatrix} \mathbf{R}_\phi^{\mathrm{T}} \mathbf{R}_\phi \begin{pmatrix} H_1 \\ H_2 \end{pmatrix} \qquad (6)$$

where $E_S = E_1 + E_2$ and $\mathbf{R}_\phi$ is, once again, a complex transformation. This time we look for an $\mathbf{R}_\phi$ that transform the magnetic field $\mathbf{H}'$ in order to obtain the desired E_S. This leads to the series impedance

$$Z_S = \frac{Z_2 + Z_1}{2\,\sin\phi} \qquad (7)$$

A similar transformation immediately follows for the parallel equivalent. In an array of parallel resistors we add currents, multiply by the common voltage, and proceed to obtain the equivalent resistance. The analogy suggests that parallel impedance can be obtained by adding magnetic fields, $H_P = H_1 + H_2$, then looking for the appropriate electric field $\mathbf{E}'$ that produce the desired H_P. This results in the parallel impedance

$$Z_P = \frac{2Z_1Z_2\sin\phi}{Z_2 + Z_1} \qquad (8)$$

At this point, the four elements of the original tensor have been transformed into four complex parameters, that is

$$\{Z_{xx},\;\; Z_{xy},\;\; Z_{yx},\;\; Z_{yy}\} \Leftrightarrow \{Z_S,\;\; Z_P,\;\; \theta_e,\;\; \theta_h\} \qquad (9)$$

Romo et al. (2004) found more convenient to substitute the angular functions θ_e , θ_h by their average $\bar{\theta}$ and their difference $\Delta\theta$, so that

$$\{Z_{xx},\;\; Z_{xy},\;\; Z_{yx},\;\; Z_{yy}\} \Leftrightarrow \{Z_S,\;\; Z_P,\;\; \bar{\theta},\;\; \Delta\theta\} \qquad (10)$$

The explicit equations represented in (10) are

$$\begin{aligned} Z_S &= \left(\frac{Z_{xx}^2 + Z_{xy}^2 + Z_{yy}^2 + Z_{yx}^2}{2} \right)^{1/2}, \\ Z_P &= \sqrt{2}\;\frac{Z_{yx}Z_{xy} - Z_{xx}Z_{yy}}{\left(Z_{xx}^2 + Z_{xy}^2 + Z_{yy}^2 + Z_{yx}^2\right)^{1/2}}, \\ \bar{\theta} &= \frac{1}{2}\arctan\left(\frac{Z_{yy} - Z_{xx}}{Z_{xy} + Z_{yx}} \right), \qquad \text{and} \\ \Delta\theta &= \arctan\left(\frac{Z_{xx} + Z_{yy}}{Z_{xy} - Z_{yx}} \right). \end{aligned} \qquad (11)$$

The four complex parameters given in (11) are a complete representation of the original tensor; in fact, an inverse transformation is also formulated in Romo et al. (2004). In contrast with ad-hoc techniques proposed to "reduce" the tensor to one suitable for 2-D interpretation (Bahr, 1988; Groom and Bailey, 1989), where information loss is inevitable because of the optimization process involved, the S-P approach is a mathematical transformation that keep intact the whole information contained in the four original tensor elements. Moreover, the new set of response functions (10) is totally valid regardless of dimensionality. Like the original tensor, it contains information of the whole current system in a general 3-D earth. However, this information, we believe, is better organized in the S-P set that it is in the original tensor, as it is represented by only two complementary impedances, accompanied by a pair of angular functions related to the geometry of the structure. It is worth to emphasize some additional properties that make Z_S and Z_P an interesting and useful pair of response functions.

The S-P impedances complement each other in a similar way as TE-TM modes complement in 2-D. Equations (7) and (8) show that series response is more sensible to the largest impedance, as the parallel one is to the smallest, just as it happens in the circuit analogy. This complementary behavior is directly connected with the different sensitivity of S-P responses to currents along and across interfaces. The series impedance is mainly affected by charge-building galvanic effects related with current flow across interfaces, while the parallel impedance is more sensitive to the inductive effect of current flow along interfaces. In that way the series equivalent behaves like TM and the parallel counterpart like TE, so extending to 3-D familiar interpretational concepts currently used in 2-D.

A most convenient property of Z_S, Z_P is that they do not depend on the measuring axes, as do the individual tensor elements, as well as the TE and TM impedances. The directional sensitivity of the new representation shifts to the angular average $\overline{\theta}$, as the angular difference $\Delta\theta$ is also rotation-invariant. This property sets aside the delicate task of pre-selecting structure azimuths.

In addition, the new response functions are more robust than the original tensor elements, as they are averages of them. We have found that when used in 2-D inversion algorithms, they are easier to fit than TE-TM impedances. Because the particular average involved in the definition of S-P impedances (eqs. 7 and 8), the resulting S-P apparent resistivity curves are close each other than TE-TM curves are. Thus, an additional benefit is that the static shift distortion present in the TE-TM curves is significantly reduced simply because of the average involved in the S-P curves. As the magnitude of the static shift is reduced, it is easier to deal with. In fact, an appropriate discretization of our models at shallow levels was enough to produce model-response curves fitting the observed shift in the S-P apparent resistivity curves.

Figure 1 shows apparent resistivity and phase curves obtained from the four elements of the original tensor as compared to the series and parallel responses, for a given MT observation site. The S-P responses consist in two apparent resistivity and phase curves, as well as two complex angular functions.

4. 2-D INVERSION OF S-P DATA

The S-P parameters are simple functions of the original tensor elements, as shown by equation (11), thus it is easy to calculate their partial derivatives with respect to model parameters. This makes it possible for existing inverse codes to be readily transformed into corresponding inverse codes for S-P data. Romo et al. (2004) validated the 2-D inversion of S-P data by adapting the Gauss-Newton inversion algorithm by Rodi and Mackie (2001) and applied it to both, synthetic and field data.

In this work we applied the same algorithm to MT data from Las Tres Vírgenes geothermal field (LTVGF), in Baja Calfornia Sur, Mexico (Figure 2). LTVGF is located in the Santa Rosalía Basin, a Plio-Quaternary depression tectonically related with the Gulf of California Extensional Province. Fault systems caused by the transtensive regime associated with the active Pacific-NorthAmerica plate boundary facilitated the emplacement of eruptive centers during Quaternary time (López *et al*., 1998). Three major volcanic centers were formed: La Reforma Caldera ~ 1.2 Ma (Sawlan, 1986), El Aguajito Complex ~ 0.8 Ma (Garduño et al., 1993) and Las Tres Vírgenes Complex 6615 yr B.P. (Capra et al., 1998).

The basement in the Santa Rosalía basin is found at 900-1000 m depth, it consists of granodioritic instrusive rocks associated with the Peninsular Range Batholith (84-91 Ma). Overlaying the basement there is a ~750 m-thick volcano-sedimentary sequence (Comondú Group) followed by a sequence of andesitic lava flows and pyroclastic products (Santa Lucía Fm.) with variable thickness. The basin is filled up with shallow-water marine deposits characterized by fossiliferous sandstones. At the top of the sequence it lays a variety of pyroclastic products related to different stages of the Quaternary volcanism.

The filed is producing geothermal fluid from localized zones with high pressure (~120 bar) and temperature over 250° at ~1200 m depth, where secondary-permeability exist because intense fracturing of the granodioritic basement. The probable heat source is a shallow magma chamber beneath La Virgen volcano.

Comisión Federal de Electricidad (CFE) started geothermal exploration at Las Tres Vírgenes in 1982, and drilled the first exploration well there in 1986. Up to date, four production wells and two injection wells have been drilled, and two 5-MW condensing turbines were installed (Quijano-León and Gutiérrez-Negrín, 2003). Steam production during 2002 was 280×10^6 kg, at an average annual rate of 37 t/h, with a total generation of 19 GWh.. The produced electricity distributes to nearby towns, which are isolated from Mexico's national electrical grid.

The MT data used in this work were measured several years ago during early exploration surveys (Vázquez et al., 1992; Romo et al., 1994). The sites are distributed over an area of ~ 400 km². Data sites along profiles AA' and BB' (Figure 2) were transformed to S-P impedances and interpreted using an adapted 2-D inversion algorithm (Romo et al., 2004).

The inversion algorithm starts comparing the response of a homogeneous earth to the observed data, then iteratively modify the model resistivity distribution, as it is required to fit the calculated response to the observed data at each site on the profile. We used a regularization approach, in other words, a pre-decided tradeoff between data fit and model smoothness is satisfied (Rodi and Mackie, 2001).

The resulting resistivity cross-section for Profile AA' is shown in Figure 3. The average misfit between model response and observed data is 17.3 %. The largest misfit is ~6 standard deviations (sd) at site 21. As 5 % uncertainty was assumed for all the observations, this is equivalent to 30 % misfit. The resistivity distribution shows a high conductivity anomaly at ~5 km depth beneath sites 21 to 88, possibly related with a relatively shallow source of heat and/or saline fluids. The elongated shape deepening vertically is probably an artifact of the methodology, as electromagnetic waves are heavily attenuated bellow the high conductivity zone. As usual in the MT practice, a given anomaly is properly resolved when the anomaly conductance σh is greater than the conductance of the media above it. Hence, resolution decreases beneath high conductivity bodies, whereas tops of conductors are well resolved when covered by more resistive layers.

The bottom panel of Figure 3 shows a layer-shaped conductive anomaly probably associated with the andesitic flows and pyroclastic products of Santa Lucía formation. This anomaly gets shallow toward the location of well LV-1 and it is in good agreement with the rock types cut by the drill. Resistivity increases with depth, as the granodioritic basement become closer.

Figurre 4 shows the resistivity cross-section for Profile BB'. In this case the average misfit between model response and observations is 13.3 %. The largest misfit is ~4.3 standard deviations (sd) at site 64, equivalent to 21.5 % misfit. The resistivity distribution shows a high conductivity anomaly at ~12 km depth beneath sites 35 to 37 possibly related with a heat source. The anomaly does not seem to be connected with shallow conductivity anomalies, in contrast to the anomaly found in profile AA'. Again, the elongated shape deepening vertically should be interpreted with caution, as is probably an artifact of the methodology. In the bottom panel we show that the layer-shaped conductive anomaly is in good agreement with LV-4 and LV-3 drill-holes. It seems that higher conductivity is constrained to the Santa Lucía formation, contrasting with the top El Viejo formation, as well as with the Comondú Group at the bottom (~1 km), at this point the resistivity begins to increase with depth as it comes into the granodioritic basement. The conductive anomaly gets thicker and deepens toward NE. At the location of LV-7 the upper-most relatively resistive zone correlates with rocks of the Santa Lucia formation, while Comodú Group and granodiorite basement are indistinguishable each other, as they are included in the high conductivity anomaly.

5. CONCLUSIONS

The new series and parallel response functions of the magnetotelluric impedance tensor, are expected to find special application in regions of complex geology like those found in geothermal and volcanic areas. In these cases the traditional TE-TM approach is often oversimplified by choosing only one polarization mode, usually TM, and basing the interpretation on the model that better fit this response alone. The series and parallel responses can be readily calculated from the original tensor and are also straightforwardly inverted using 2-D software. The example discussed from Las Tres Virgenes geothermal illustrates the application of this approach. The results are encouraging given the correlation of the inverted models with what is known of the subsurface geology.

ACKNOWLEGMENTS

The authors appreciate the drill-hole information provided by Gerencia de Proyectos Geotermoeléctricos of CFE (GPG). The MT data used for this paper were surveyed by CICESE under contract for GPG in 1992 and 1994.

REFERENCES

Bahr, K.: Interpretation of the magnetotelluric impedance tensor: regional induction and local telluric distortion, *J. Geophys.*, **62** (1988), 119-424.

Capra, L., Macías, J.L, Espíndola, J.M., and Siebe, C.: Holocene plinian eruption of La Virgen volcano, Baja California, México, *Jour. Volcanol. and Geothermal Res*., **80**, (1998), 239-266.

deGroot-Hedlin, C. and Constable, S.: Occam's inversion to generate smooth two-dimensional models for magnetotelluric data, *Geophysics*, **55**, (1990),1613-1624

deGroot-Hedlin, C. and Constable, S.: Inversion of magnetotelluric data for 2-D structure with sharp resistivity contrasts, *Geophysics*, **69**, (2004), 78-86.

Garduño-Monroy, V.H., Vargas-Ledezma, H., Campos-Enriquez, J.O.: Preliminary geologic studies of Sierra El Aguajito (Baja California, México): a resurgent-type caldera, *Jour. Volcanol. and Geothermal Res*., **59**, (1993), 47-58.

Groom, R.W. and Bailey, R.C.: Decomposition of magnetotelluric impedance tensor in presence of local three-dimensional galvanic distorsion, *J. Geophys. Res*., **94**, (1989), 1913-1925.

López, A.: Síntesis geológica de la zona geotérmica de Las Tres Vírgenes, B.C.S., México, *Geotermia Rev. Mex. Geoenerg.*, **14**, (1998), 3-14.

Newman, G. and Alumbaugh D.: Three-dimensional magnetotelluric inversion using non-linear conjugate gradients, *Geophysical Jour. International*, **140** (2000), 410-424.

Ogawa, Y. and Uchida, T.: A two-dimensional magnetotelluric inversion assuming Gaussian static shift. *Geophysical Jour. International*, **126**, (1996), 69-76.

Quijano-León, J.L. and Gutiérrez-Negrín, L.C.A.: 30 years of geothermal-electric generation in Mexico, *GRC Bull*., **32**, (2003), 198-203.

Rodi, W., and Mackie, R.L.: Nonlinear conjugate gradients algorithm for 2-D magnetotelluric inversion. *Geophysics*, **66**, (2001), 174-187.

Romo, J. M., Flores, C., Vega, R., Esparza F., and Gómez, E.: Estudio magnetotelúrico en el área geotérmica Tres Vírgenes-Aguajito, B.C.S.: Informe de Interpretación, *Intern, Rep., Contract CLS-GPG-4003-94/CFE-CICESE, GPG-CFE*, (1994), 527 pp.

Romo, J.M., Gómez-Treviño E. and Esparza E.: Series and parallel transformation of the magnetotelluric impedance tensor: theory and applications, *Phys. Earth Planet. Int.*, (2004), in press.

Sasaki, Y.: 3-D inversion of electrical and electromagnetic data on PC. *Proc. Second Int. Symposium on Three-Dimensional Electromagnetics*, (1999), 128-131.

Sasaki, Y.: Three-dimensional inversion of static-shifted magnetotelluric data. *Proc. 5th SEGJ Int. Symposium* (2001), 185-190.

Sawlan, M.G.: Petrogenesis of Late Cenozoic volcanic rocks from Baja California Sur, México. PhD Thesis, University of California, Santa Cruz, (1986), 174 pp.

Siripunvaraporn, W. and Egbert, G.: An efficient data-subspace inversion method for 2-D magnetotelluric data, *Geophysics*, **65**, (2000), 791-803.

Smith, J.T. and Booker, J.R.: Rapid inversion of two- and three-dimensional magnetotelluric data, *J. Geophys. Res*., **96-B3**, (1991), 3905-3922.

Uchida, T. and Sasaki, Y.: Stable 3-D inversion of MT data and its application to geothermal exploration, *3D-EM-III Workshop*, (2003).

Uchida, T.: Smooth 2-D inversion for magnetotelluric data based on statistical criterion ABIC, *J. Geomag. Geolelectr*., **45**, (1993), 841-858.

Vázquez, R., Vega, R., Herrera, F., and López, A.: Evaluación con métodos electromagnéticos del campo geotérmico de Tres Vírgenes, B. C. S., Primera etapa, *Intern. Rep. Contract CLS-GPG-003-94/CFE-CICESE, GPG-CFE*, (1992), 175 pp.

Zhdanov, M.S., Fang, S. and Hursin, G.: Electromagnetic inversion using quasi-linear approximation, *Geophysics*, **65**, (2000), 1501-1513.

.

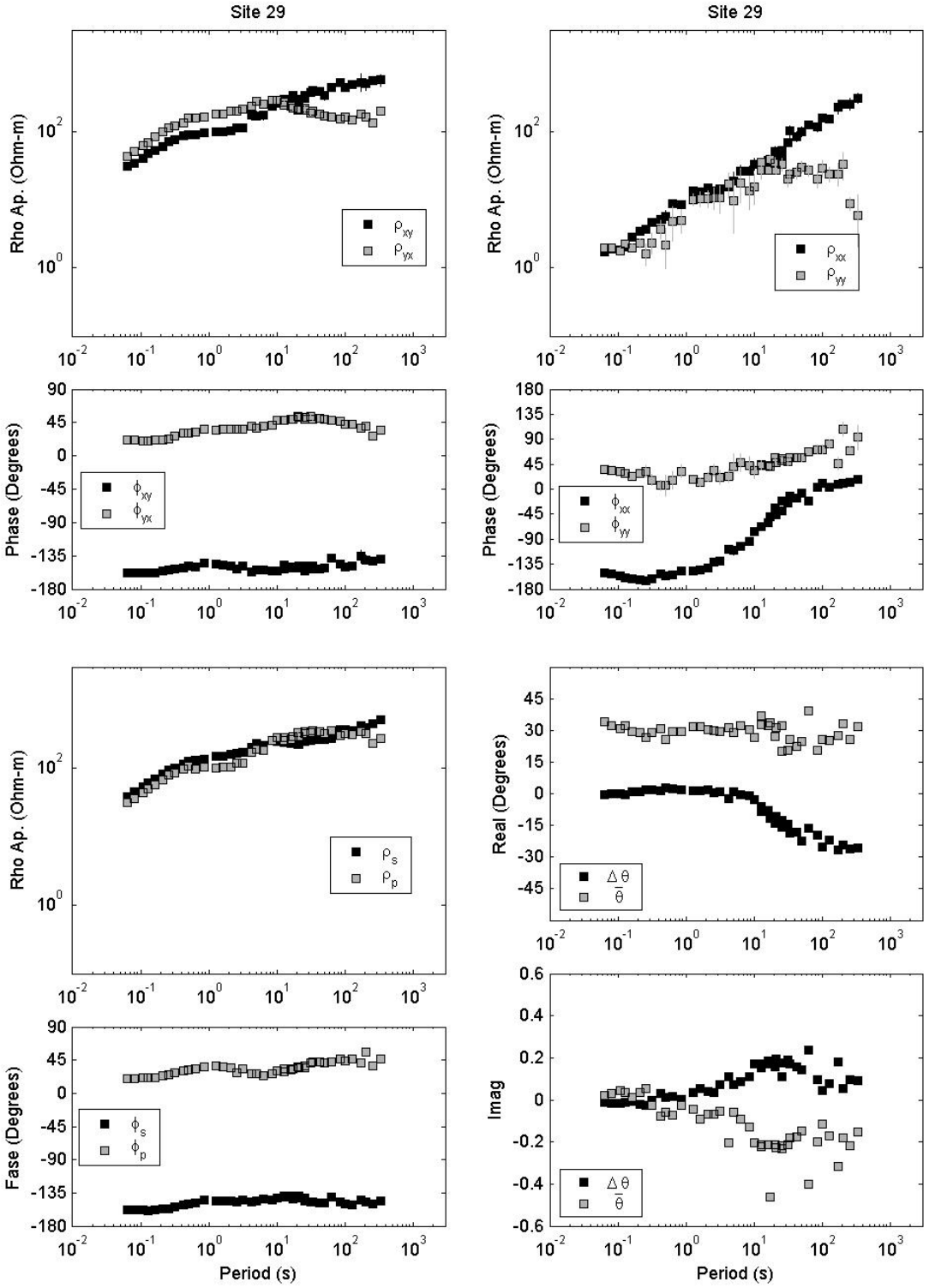

Figure 1: Apparent resistivity and phase curves from the four elements of the original tensor as compared with series and parallel response functions: two apparent resistivity and phase curve and two complex angular functions.

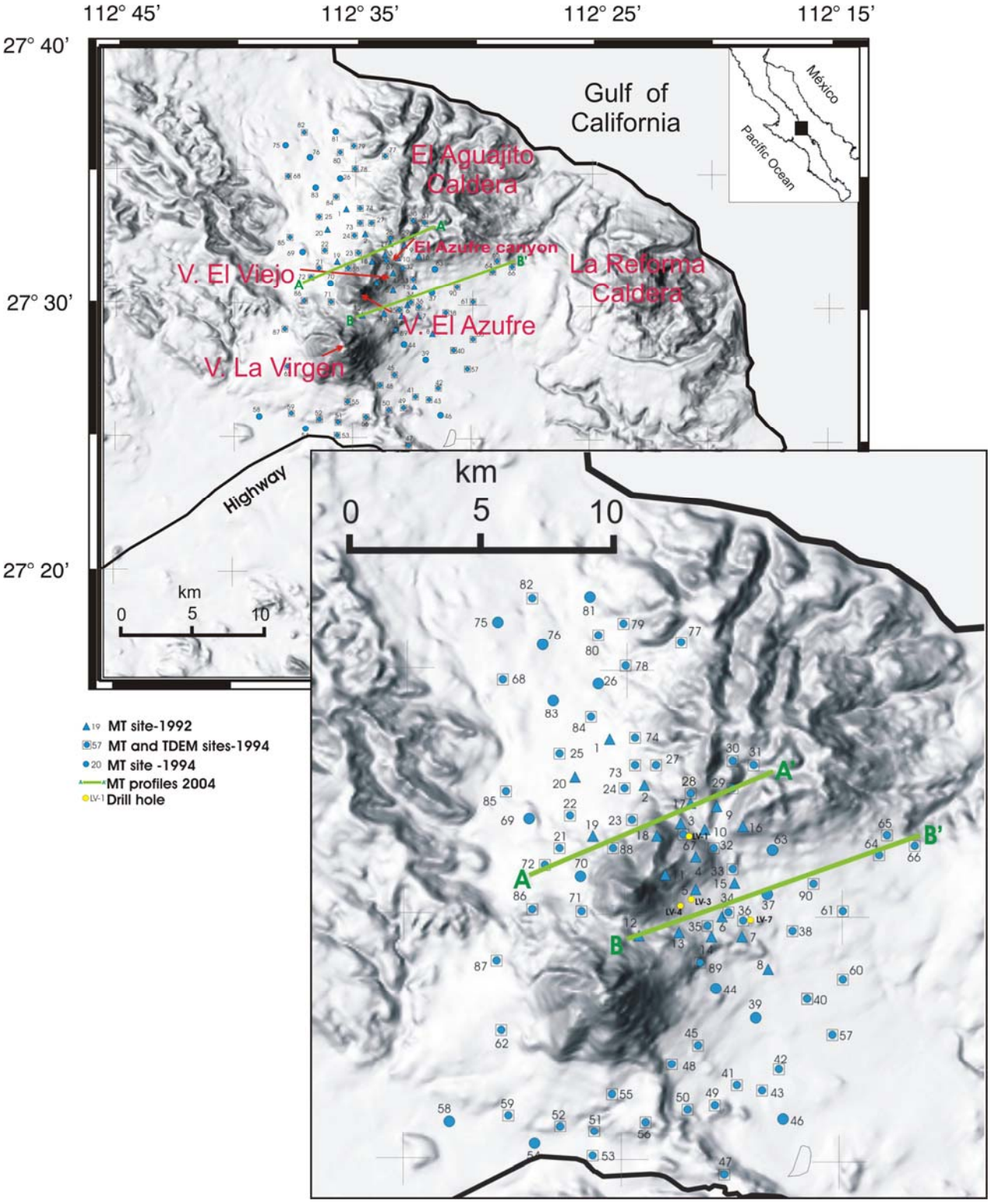

Figure 2: Geographical location of LTVGF with main volcanic structures. Location of MT observation sites. Location Profiles AA' and BB' processed for this work.

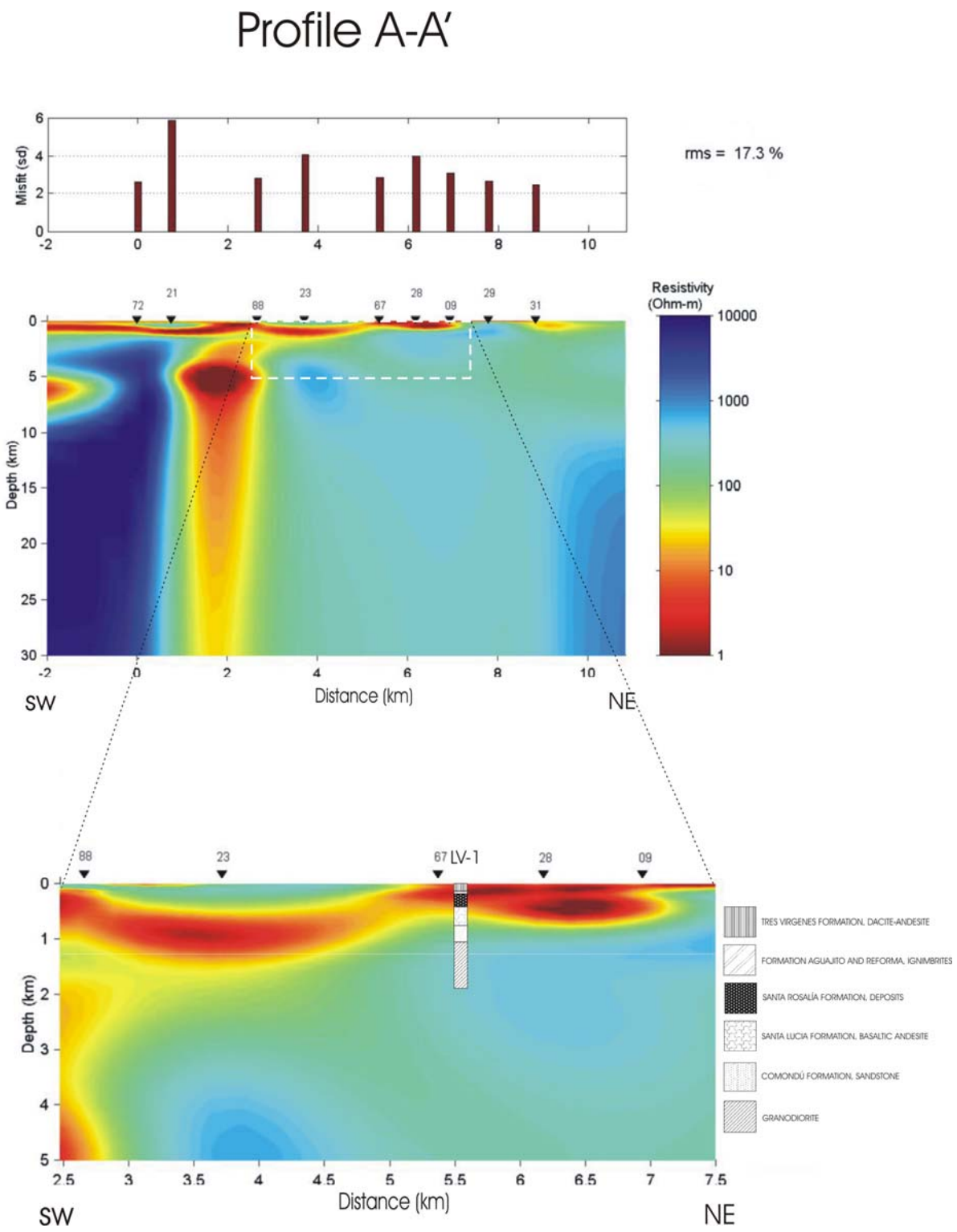

Figure 3: Profile AA'. Subsurface resistivity cross-section obtained after 2-D inversion of S-P impedances. The bar-plot at the top panel shows the misfit between observed and calculated curves at every data site (triangles). The middle panel shows the resistivity distribution beneath the profile. Bottom panel shows the correlation with lithology in nearby drill-holes.

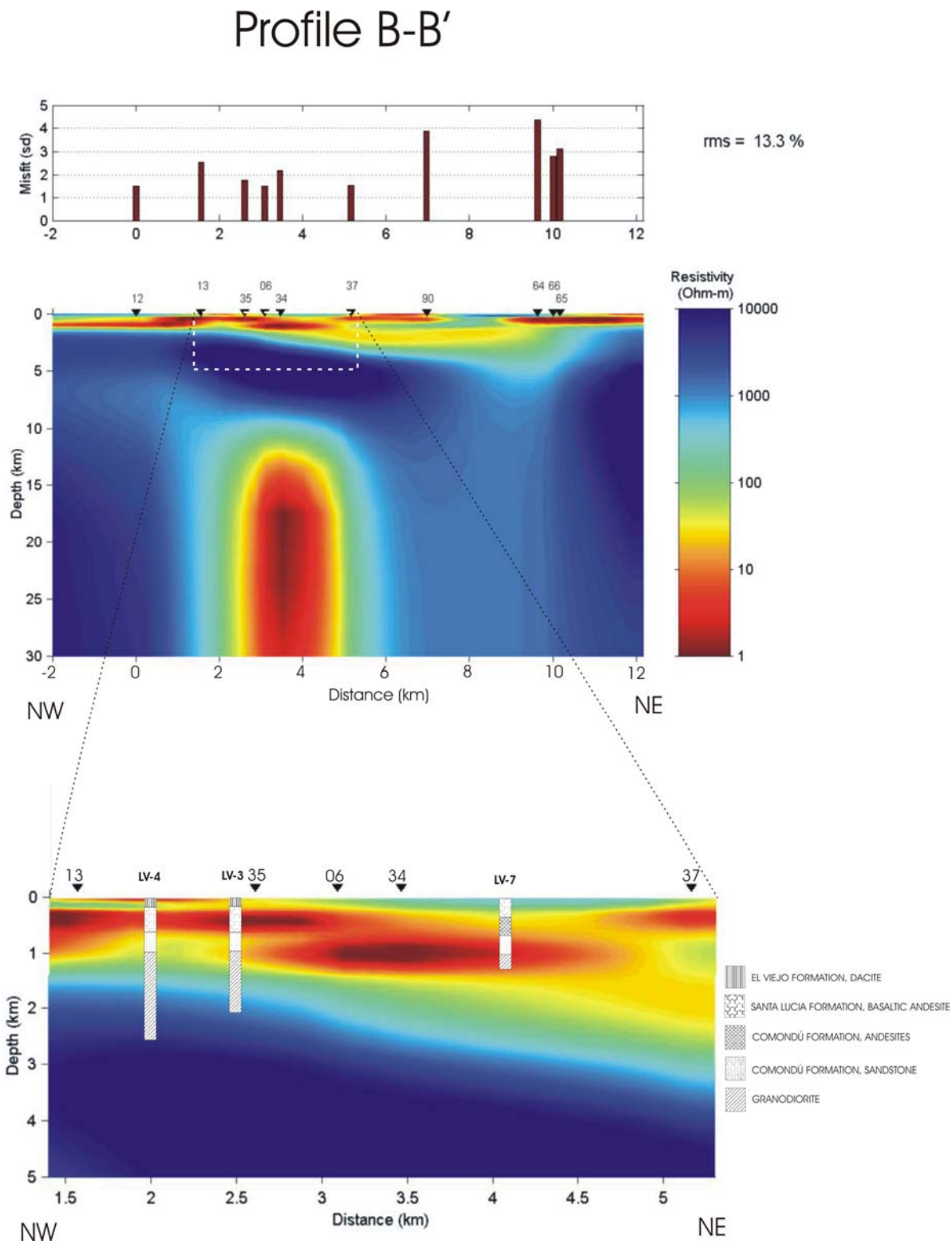

Figure 4: Profile BB'. Subsurface resistivity cross-section obtained after 2-D inversion of S-P impedances. The bar-plot at the top panel shows the misfit between observed and calculated curves at every data site (triangles). The middle panel shows the resistivity distribution beneath the profile. Bottom panel shows the correlation with lithology in nearby drill-holes.